Path-related unexpected injection charges in $BaTiO_3$ ferroelectric thin films studied by Kelvin force microscopy

Huifen Guo, Gang Cheng, Shujie Wang, Shuxi Dai, Sixin Wu, Shaomin Zhou, Yuncai Li, and Zuliang Du[a)]
Key Laboratory for Special Functional Materials of the Ministry of Education, Henan University, Kaifeng 475004, People's Republic of China

(Received 13 August 2009; accepted 18 September 2010; published online 18 October 2010)

The collective effect of injection charges constructed in a dot array using scanning probe microscopy (SPM) in $BaTiO_3$ ferroelectric thin films was investigated with Kelvin force microscopy (KFM). Unexpected charges were observed in the SPM tip paths where poling bias was zero. The analysis of the array with different poling biases shows that the collective effect of the injection charges in the dot array induced a potential difference between film and tip, which in turn injected unexpected charges. The calculated potential difference distribution along the tip's paths correlates well with KFM images of the unexpected charges. © *2010 American Institute of Physics*. [doi:10.1063/1.3499749]

High-density nonvolatile memories that are based on modifying ferroelectric domains by scanning probe microscope (SPM) technique have been widely investigated due to their superior lateral resolution, nondestructiveness, and easy manipulation for polarization.[1–3] Generally, the polarization states are manipulated by applying a dc poling bias between the film and the conductive tip of the SPM. During this process, considerable charges can be injected into the film. The field induced by these injected charges will disturb the normal polarization states and can generate serious deleterious effects on memory performance: antiparallel polarization, which leads to bit error in memories[4–6] and polarization fatigue which shortens memory lifetime.[7,8]

The effects of injection charges during the polarization process using the SPM technique have been intensively investigated using electric force microscopy (EFM) (Ref. 4) and Kelvin force microscopy (KFM).[9] Most research has focused on disturbances in the polarization state on a single logic bit caused by the injection charges. However, in real SPM-based high-density ferroelectric memory there are a large number of logic bits and injection charges may exist in all of them. Therefore, it is necessary to investigate the collective effect of all the injection charges in a bit array.

KFM can measure surface potential distribution with micrometer resolution,[10–12] and has been widely used to observe surface charges in ferroelectric thin films.[13,14] Therefore, KFM can directly observe the spatial distribution of injection charges in a ferroelectric memory array, providing a useful tool to study the collective effect of injection charges in the array. In this paper, an array of injection charges in $BaTiO_3$ (BTO) ferroelectric thin film was constructed by SPM and the collective effect of the injection charges in the array was investigated with KFM. Some unexpected charges, which may affect the performance of ferroelectric memory, were observed in the movement paths of the SPM tip where the poling bias was zero. In addition, the generation mechanism of the unexpected charges were discussed.

The bottom electrodes of the samples used in this study were prepared by depositing $LaNiO_3$ films on $SiO_2/Si(100)$ substrates using a chemical solution technique as described by Wang *et al.*[15] Polycrystalline BTO films, approximately 120 nm thick, were deposited on the bottom electrodes by spin coating of the BTO sol.[16] The local electric poling and the surface potential measurement were performed on a multifunctional SPM (Seiko, SPA400) in ambient atmosphere. The conductive tip of the SPM was grounded. For the local poling, a dc bias was applied to the bottom electrode. For the surface potential measurement, KFM was performed using an active trace mode.[10]

Figure 1 shows the topography (a) and surface potential (b) images of the BTO thin film obtained simultaneously by KFM after the poling of nine 0.5×0.5 μm^2 squares with various negative poling biases. The tip scanned in contact mode with a constant loading force (scan speed of 10 Hz, 256 lines) for the poling of each square. As shown in Fig. 1(b), the surface potential of all the poled squares displays bright contrast compared with the unpoled region and the bright contrast gradually increases with the absolute value of poling bias. In the surface potential image, the bright contrast represents the higher surface potential induced by positive charges. On the other hand, the dark contrast represents the

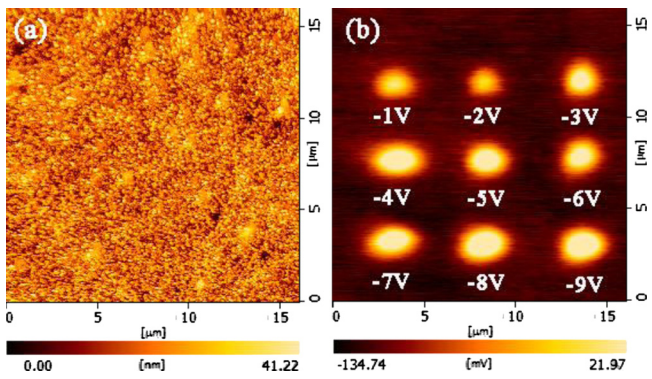

FIG. 1. (Color online) (a) Topography image and (b) surface potential image of the BTO film obtained after the poling of nine 0.5×0.5 μm^2 squares with various negative biases.

[a)]Author to whom correspondence should be addressed. Electronic mail: zld@henu.edu.cn.

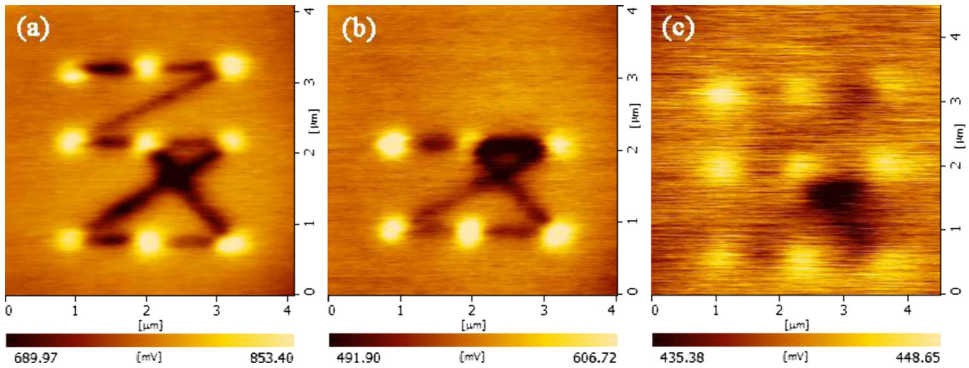

FIG. 2. (Color online) Surface potential images of the BTO film after the poling of a nine-dot array shown in Fig. 3(a). The pulse biases of the nine dots in 2(a) and 2(c) are −9.9 V and −6 V, respectively. In 2(b), the pulse bias of the first three dots is 0 V, and for the following six dots, bias is −9.9 V.

lower surface potential induced by negative charges. When the negative poling bias is applied to the bottom electrode, two types of charges can be induced at the surface of the poled region:[14,17] the first is negative polarization charges in the BTO film surface; the second type is free charges, including positive injection charges, internal charges and/or charges from the ambient, which can be transferred to the BTO film surface and be trapped in the poled region. When the positive injection charges are dominant, the surface potential of the poled square is higher than that of the unpoled region and gradually increases with the absolute value of the poling bias.[18] Therefore, the positive charges in the poled region in Fig. 1(b) are dominated by the injection charges.

Figure 2(a) shows the surface potential image of a nine-dot array measured by KFM immediately after poling by the conductive tip in contact mode. The sketch map of the poling process is shown in Fig. 3(a). As the tip moved to the positions marked as solid dots numbered 1 to 9 [Fig. 3(a)], a −9.9 V pulse bias of 10 s was applied at the bottom electrode. The tip subsequently moved to the next dot along the arrow. The poling bias was turned off when the tip moved between two dots along the path marked as a line with an arrow [Fig. 3(a)]. The tip scanned using the contact mode during the entire poling process, where the loading force and the tip speed were kept constant at 1 nN and 0.1 μm/s, respectively. Here, $P_{m,n}$ is defined as the movement path from dot m to dot n. As mentioned in Fig. 1(b), the bright contrast of the nine dots in Fig. 2(a) corresponds to the positive injection charges induced by the −9.9 V pulse bias. However, unexpected clear dark contrasts are observed in all of the tip's movement paths where poling bias was not applied, indicating the presence of negative charges. A similar phenomenon is observed when the nine-dot array was poled with a positive pulse bias. In this situation, the negative injection charges are shown in the nine dots and positive charges are observed unexpectedly in the tip's movement paths [see Ref. 19]. Clearly, the unexpected charges have an opposite polarity to the injection charges in the corresponding dot array. The control experiment with different tip movement paths further confirmed that the unexpected charges always appear in the movement paths of the tip [see Ref. 19]. To distinguish between the injection charges in the dots caused by the poling pulse bias and the charges in the movement paths, the corresponding charges in the movement paths where poling bias was not applied are referred to as unexpected charges.

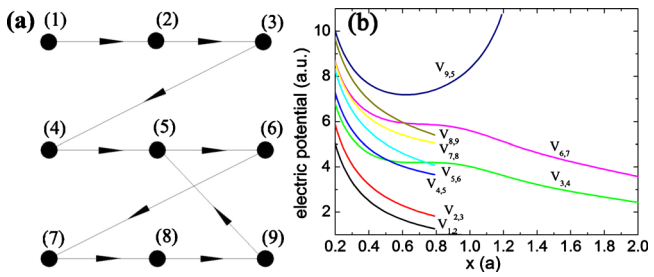

FIG. 3. (Color online) (a) Sketch map of the poling process. The solid dots denote the locations of poling bias application and the lines with arrows denote the movement paths of the tip without poling bias. (b) The calculated potential distributions along the nine movement paths by the positive injection charges in the dots.

Figure 2(b) shows the surface potential image of a dot array poled with the same poling parameters as those indicated in Fig. 2(a), with the exception of the first three dots (dots 1–3) whose poling pulse bias was set at 0 V. In Fig. 2(b), no injection charges were present in dots 1–3 where 0 V pulse bias was applied and unexpected charges were not observed in the corresponding tip movement paths ($P_{1,2}$, $P_{2,3}$, and $P_{3,4}$). After the positive charges had been injected by a −9.9 V pulse bias in dot 4, the negative unexpected charges were observed again in the following tip movement paths. In the two poling processes in Figs. 2(a) and 2(b), the loading force between the SPM tip and the film is the same. Therefore, the unexpected charges were not caused by the loading force, but by the injection charges in the dots.

In the poling process of the nine-dot array, the charges in the dots were injected along the tip movement paths. These injection charges induced the potential and caused the potential difference between the film and the grounded tip. With this potential difference, the free charges could be injected into the film by the grounded tip during the tip movement. Therefore, the potential difference between the film and the grounded tip, induced by the injection charges in the dots, might be the main reason for the generation of the unexpected charges. In Fig. 2(a), the positive injection charges in the dots induced a positive potential around each dot, causing a positive potential difference between the film and the grounded tip. With this positive potential difference, the negative charges were injected into the film during the tip movement. These charges correspond to the dark contrast areas in the tip movement paths of the KFM image.

As discussed above, the unexpected charges were injected by the potential difference between the film and the grounded tip, induced by the injection charges in the dots. The quantity of injected charge increased with the absolute value of the potential difference between film and tip. Therefore, with the increase in quantity of injection charge in the dots, the corresponding absolute value of the potential differ-

ence between film and tip should increase. Conversely, with the decrease in quantity, the absolute value should decrease. The unexpected charges injected in the tip movement paths should increase or decrease accordingly. Figure 2(c) shows the KFM image of another nine-dot array in which the poling bias was −6 V. The other poling parameters are the same as those indicated in Fig. 2(a). Compared with Fig. 2(a), the absolute value of the poling bias in Fig. 2(c) is lesser and, as a result, the quantity of injection charge in the nine dots and the quantity of unexpected charge injected in the tip movement paths decreased in a consistent manner with the relationship between injection charge in the dots and unexpected charge as discussed above.

In each of the experiments, such as those shown in Figs. 2(a) and 2(c) and the control experiment [see Ref. 19], the nine-dot arrays were constructed by a constant poling bias following the poling process indicated in Fig. 3(a). In most of the experiments, the quantity of unexpected charge in $P_{6,7}$ and $P_{9,5}$ is higher than in the other tip movement paths. This path-related behavior of the unexpected charges is attributed to the different potential differences in different tip movement paths. The potential difference in any tip movement path is induced by the collective effect of all the existing injection charges around this movement path. In addition, for different movement paths, the distribution of the existing injection charges in the dot array is different. For example, the injection charge in the first dot (dot 1) is the only injection charge that affected the potential difference between the film and tip in $P_{1,2}$, while for $P_{9,5}$, injection charges were present in all nine dots. Therefore, the absolute value of the potential difference in $P_{9,5}$ was higher than that of $P_{1,2}$, resulting in a higher quantity of unexpected charge injected into $P_{9,5}$ compared with that of $P_{1,2}$.

Due to the grounded tip, the resulting potential difference between film and tip was equal to the corresponding potential. To verify the path-related behavior, we calculated the potential distributions induced by the collective effect of the injection charges in the dots along the different tip movement paths as indicated in Fig. 3(a). The potential distribution of $P_{m,n}$ is defined as $V_{m,n}(x)$, in which x denotes the distance from dot m to any position in $P_{m,n}$. According to the construction process, $V_{m,n}(x)$ was attributed to the superposition of potentials induced by the injection charges in the dots marked with numbers 1 to m. The potential calculation was based on Coulomb's law, the injection charges in the dots were assumed to be an ideal positive point charge, and the quantity of injection charge was assumed equal in every dot of the array. The detailed calculations of the potential distributions are shown in Ref. 19. Figure 3(b) shows the corresponding calculated potential distributions, drawn according to the calculated expressions in Ref. 19, in which " a " denotes the distance between two adjacent dots. It is clearly indicated that $V_{9,5}(x)$ and $V_{6,7}(x)$ are higher potentials than the ones seen in the other movement paths. These results are in agreement with the experimental results, confirming the path-related behavior of the unexpected charges. Remarkably, for a real poling process, the quantity of injection charge in the dots and the quantity of unexpected charge in the tip movement paths could be affected by other factors, such as nonuniformity in thickness, particle size in the film, and contact quality between tip and film, etc. In addition, the unexpected charges can also weaken and disturb the potential distribution along the tip movement paths. Their effects on the quantity of the unexpected charge need further investigation.

In summary, the collective effect of injection charges in the dot arrays during the poling process of ferroelectric thin films was investigated. Path-related unexpected injection charges were observed by KFM in the movement paths of the SPM tip where the unexpected charges were observed to have the opposite polarity to the injection charges in the dots. These unexpected charges are attributed to the collective effect of the injection charges in the dots, as confirmed by the calculation result of the potential difference distribution along the tip movement paths. Obviously, this effect must be taken into account during the scan-writing process in high-density ferroelectric memory based on SPM technology because the effect directly limits memory density. Moreover, understanding path-related unexpected injection charges will help minimize or avoid this effect by optimizing tip paths, thus increasing memory density.

This work was supported by the National Natural Science Foundation of China (Grant Nos. 10874040 and 60906056) and the Cultivation Fund of the Key Scientific and Technical Innovation Project, Ministry of Education of China (Grant No. 708062). Thank Professor Jun Wang of Shanghai University and Professor Jin Zhang of Peking University very much for help on experiments.

[1] C. H. Ahn, T. Tybell, L. Antognazza, K. Char, R. H. Hammond, M. R. Beasley, Ø. Fischer, and J.-M. Triscone, Science **276**, 1100 (1997).
[2] P. Paruch, T. Tybell, and J.-M. Triscone, Appl. Phys. Lett. **79**, 530 (2001).
[3] J. Y. Son, C. S. Park, S.-K. Kim, and Y.-H. Shin, J. Appl. Phys. **104**, 064101 (2008).
[4] S. Bühlmann, E. Colla, and P. Muralt, Phys. Rev. B **72**, 214120 (2005).
[5] Y. Kim, S. Bühlmann, S. Hong, S.-H. Kim, and K. No, Appl. Phys. Lett. **90**, 072910 (2007).
[6] A. L. Kholkin, I. K. Bdikin, V. V. Shvartsman, and N. A. Pertsev, Nanotechnology **18**, 095502 (2007).
[7] X. J. Lou, M. Zhang, S. A. T. Redfern, and J. F. Scott, Phys. Rev. B **75**, 224104 (2007).
[8] A. Q. Jiang, Y. Y. Lin, and T. A. Tang, J. Appl. Phys. **102**, 074109 (2007).
[9] J. Y. Son, K. Kyhm, and J. H. Cho, Appl. Phys. Lett. **89**, 092907 (2006).
[10] H. O. Jacobs, H. F. Knapp, and A. Stemmer, Rev. Sci. Instrum. **70**, 1756 (1999).
[11] S. J. Wang, G. Cheng, X. H. Jiang, Y. C. Li, Y. B. Huang, and Z. L. Du, Appl. Phys. Lett. **88**, 212108 (2006).
[12] G. Cheng, S. J. Wang, K. Cheng, X. H. Jiang, L. X. Wang, L. S. Li, Z. L. Du, and G. T. Zou, Appl. Phys. Lett. **92**, 223116 (2008).
[13] X. Q. Chen, H. Yamada, T. Horiuchi, K. Matsushige, S. Watanabe, M. Kawai, and P. S. Weiss, J. Vac. Sci. Technol. B **17**, 1930 (1999).
[14] J. Y. Son, S. H. Bang, and J. H. Cho, Appl. Phys. Lett. **82**, 3505 (2003).
[15] G. S. Wang, Q. Zhao, X. J. Meng, J. H. Chu, and D. Rémiens, J. Cryst. Growth **277**, 450 (2005).
[16] H. Basantakumar Sharma and H. N. K. Sarma, Thin Solid Films **330**, 178 (1998).
[17] J. Y. Son, B. G. Kim, C. H. Kim, and J. H. Cho, Appl. Phys. Lett. **84**, 4971 (2004).
[18] Y. Kim, C. Bae, K. Ryu, H. Ko, Y. K. Kim, S. Hong, and H. Shin, Appl. Phys. Lett. **94**, 032907 (2009).
[19] See supplementary material at http://dx.doi.org/10.1063/1.3499749 for (1) the control experiments and (2) the detailed calculation expressions of the potential distributions.